LIFE12 ENV/CY/544: Sustainable management of livestock waste for the removal/recovery of nutrients

Sono-Chemical Reactor Design for Biodiesel Production via Transesterification

CYPRUS 2016, 4th International Conference on Sustainable Solid Waste Management, 23rd- 25th June 2016, Limassol, Cyprus
www.cyprus2016.uest.gr, www.livewaste.org

Mohammed Noorul Hussain (mhussain1@masdar.ac.ae), Isam Janajreh (ijanajreh@masdar.ac.ae*)
Mechanical and Materials Engineering Department
Masdar Institute of Science and Technology, P.O. Box 54224

ABSTRACT

Biodiesel is an alternative and sustainable fuel that can reduce the dependence on fossil diesel. This commodity has not only been promoted in the developed world but also in developing countries like Indonesia, Brazil and others. Biodiesel is produced from the transesterification reaction between vegetable oils or waste cooking oils and an alcohol, in the presence of an acidic or basic catalyst. This reaction is conventionally carried out in mechanically stirred batch process. Use of ultrasound is a proven enhancement to the production process. Continuous, compact and efficient sonochemical reactors are needed to increase biodiesel production volumes. In this work simulation assisted design of a sonochemical reactor is pursued. To design the sono-chemical reactor, numerical modelling of the physical phenomena like wave propagation, attenuation, and reactive flow has been carried out. Physics governing the reactive flow circulation and simultaneous sonication in the cylindrical reactor are simulated. 2D axi-symmetric model of the proposed reactor is created. Coupled time independent wave equation with complex wave number, Navier-Stokes equation, multiple species equations and Arrhenius kinetics are solved simultaneously. A sensitivity analysis based on geometry (height and diameter), rated power and frequency is carried out, and the physical (acoustic pressure) and chemical (reactive) prospects of the reactor are studied. Results show that wave attenuation due to cavitation restricts the increase in reactor height, but not the diameter. Increase in rated power resulted in higher acoustic pressure and rate constant. Effect of frequency on the physical and chemical aspects although was positive, but the relation was not well defined. This work underlines the fundamental knowledge that required in designing effective and innovative sono-reactors.

Keywords: Transesterification, ultrasound, biodiesel, process intensification, numerical modelling.

INTRODUCTION

Transesterification reaction is a mass transfer limited reaction, which is neither strongly endothermic nor exothermic. It is a reaction between the tri-glycerides in the feedstock and an alcohol to produce fatty acid alkyl esters and glycerol. The feedstock for biodiesel can either be pure vegetable oils or used cooking oils and the alcohol is most commonly methanol. Theoretically, from the process stoichiometry, 3 moles of methanol are needed to convert 1 mole of TG to 3 moles of Fatty Acid Methyl Ester (FAME-biodiesel) and one mole of glycerol byproduct [1].

$$\text{Triglyceride} + 3\ \text{Methanol} \leftrightarrow 3\ \text{FAME} + \text{Glycerol}$$

The reaction takes place in the presence of a catalyst that can either be a homogeneous catalyst like NaOH (Sodium hydroxide) or KOH (Potassium hydroxide) or heterogeneous catalyst like CaO (Calcium oxide). Ways of making the process highly prolific and much faster, must be found to make biodiesel more economical appealing in the market. Chemical process intensification has been receiving much attention and can be applied to transesterification.

From among the multiple ways of achieving this, one way is to push the reaction parameters such as temperature and pressure to reach supercritical conditions. However the energy consumption in this process is very high due to the elevated state conditions. Sonication is another pathway for speeding and intensifying the reaction through the use of ultrasound to create pressure variations in the fluid domain which cause growth of micro-bubbles in the bulk of the fluid. These bubbles have very high internal temperature and pressure (1000K, 500atm). At relatively high ultrasonic intensities these bubbles grow rapidly and collapse violently, generating energy and mechanical/agitation effect which in turn increases the mass transfer rate at the boundary [2]. Sonication generates millions of such bubbles in the fluid, hence the combined action of the micro-level activities enhances the reaction in the complete fluid domain. This is a much simpler and energy efficient process since it localizes the temperature and pressure effect which eliminates the need of high energy input.

Compared to the conventional stirred method sonication is much advanced in terms of product proliferation and reaction time which is proven in literature. Stavarache et al. [3] reported higher yields in shorter time using ultrasonic transesterification under homogeneous catalysts of NaOH and KOH and for the same molar ratio and catalyst amount compared to conventional stirring method. Manickam et al. [4] reported that mechanical agitation method requires triple the time to give 78% yield as compared to ultrasonic transesterification which gives about 93% yield with 1% KOH and 3:1 methanol to oil molar ratio. Babajide et al. [5] reported a conversion of 96.8 % using waste cooking oil, methanol and KOH in just 30 minutes of reaction time. In this work also ultrasonic technology was used and molar ratio and catalyst % were 6:1 and 0.75 %. The amount of fatty acids present in the oil used determines the conversion percentage of fatty acid methyl esters.

Since sonication is now a proven enhancement for the biodiesel production process, there is a need for research on the design of sonochemical reactors. Design of sonochemical reactors has been studied by many researchers [6] [7] [8]. However their designs were based on batch process reactors, which can only process a small quantity of liquid in their operation time. Scaling up of such reactors requires either larger ultrasound equipment or multiple smaller ones. Both the options are energy and cost intensive. To progress to a design that is energy and cost effective one needs to move from batch type reactors to continuous reactors. The current need is a compact, continuous, sono-chemical reactor which can give good yields of biodiesel in shorter time while not consuming higher energy. Such a reactor finds applications in commercial biodiesel production due to the ease of production volume scale up and also in laboratories for research on biofuels. An efficient and compact sonochemical reactor can also find purpose in residential communities where large quantity of waste cooking oil is produced and is mostly drained/wasted. Being a potential biodiesel feedstock, waste cooking oil can be domestically processed within communities in such compact reactors, and the produced biodiesel can be used internally or sold. This takes us one step ahead in the path to achieving sustainable development.

In this work, we have modelled the physics occurring in continuous sono-chemical conversion of vegetable oil to biodiesel in a continuous sono-chemical reactor. The modelling is numerical, and has been carried out using a multiphysics, finite element based numerical package. The ultrasound wave is modelled using the Helmholtz equation. Additionally, the wave attenuation effect of the cavitation bubble cloud has also been modeled using a complex wave number for the Helmholtz equation [9]. The flow of reactants, is modelled with the laminar, incompressible, steady Navier-Stokes equations. The species transport equation is used to model and track the reactive flow. The reaction rates follow the Arrhenius kinetic equation. The kinetic reaction rate due to the flow and that due to the ultrasound have to be differentiated. Following the work of Jordens et al [10], who modelled a continuous flow sono-chemical reactor (for Carbon tetrachloride degradation), the sonication reaction rate and flow reaction rate have been coupled using a logical reaction rate coupling model based on acoustic pressure and cavitation bubble volume. With the complete mathematical setup described above, the simulation of physics has been carried out for a simple cylindrical reactor. A sensitivity analysis based on geometry (height and diameter), rated power and frequency has been carried out to investigate the physical (acoustic) and chemical (reactive) performance of the reactor.

METHODOLOGY

The analysis scheme shown in Fig.1 along with the reactor geometry.

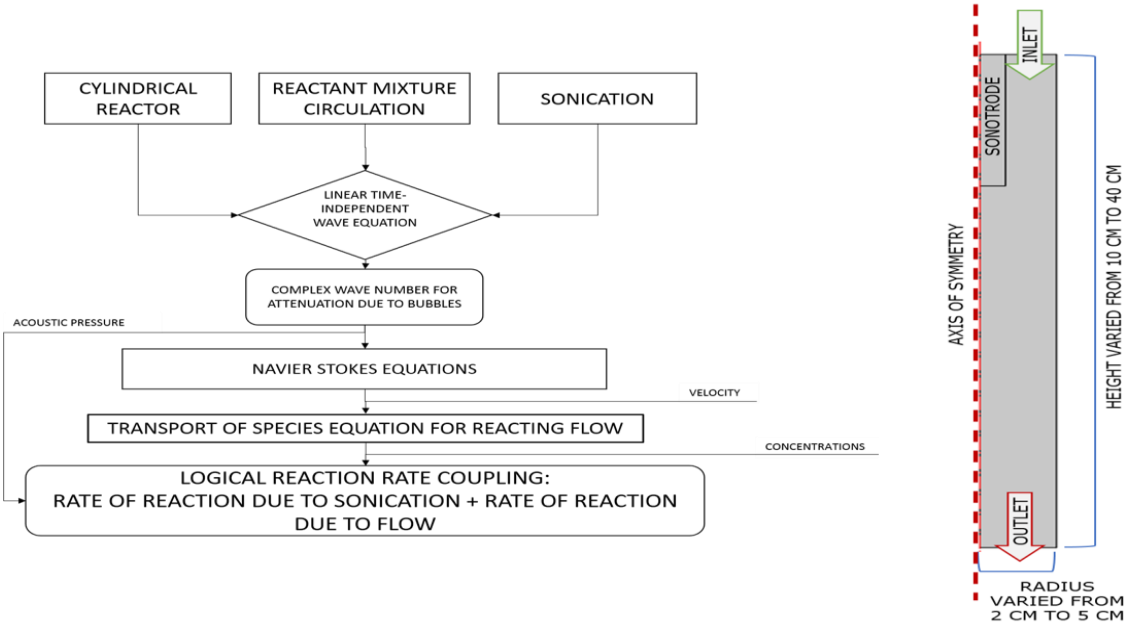

Fig.1 Schematic of analysis and reactor geometry

Helmholtz equation (linear time independent wave equation):

The Helmholtz equation is given in Eq. 2. P is the acoustic pressure and k_c is the complex wave number to account for wave attenuation due to cavitation bubbles.

$$\nabla^2 P + k_c^2 . P = 0 \tag{2}$$

Complex wave number:

The cavitation and the wave attenuation is a highly non-linear phenomena which is difficult to model. Commander and Prosperetti [11] formulated a complex wave number to linearize and simplify the modelling. It has been used in in some previous works to study the acoustic cavitation phenomena and design sono-chemical reactors [9] [10]. The complex wave number is given in Eq. 3.

$$k_c{}^2 = \frac{\omega^2}{C^2}\left(1 + \left(4\frac{\pi C^2 n_b R}{\omega_o{}^2 - \omega^2 + 2ib\omega}\right)\right. \tag{3}$$

Where ω is angular frequency ($2\pi f$), f is frequency, C is speed of sound, n_b is the number of bubbles, *R* is the bubble radius which is 3/f [10] and *b* is the damping coefficient. ω_o is the resonance frequency given as in Eq. 4.

$$\omega_o = \left(\frac{P_o}{\rho R^2}\right)\left(\mathrm{Re}(\emptyset) - \frac{2\boldsymbol{\sigma}}{R\,P_o}\right) \tag{4}$$

The undisturbed pressure P_o is given in Eq. 5.

$$P_o = P_{liq} + \frac{2\boldsymbol{\sigma}}{R} \tag{5}$$

Where $\boldsymbol{\sigma}$ the surface tension and $\emptyset$ is a complex dimensionless parameter given in Eq. 6.

$$\emptyset = \frac{3\gamma}{1 - 3(\gamma - 1)\, i\, X\, [\sqrt{\frac{i}{X}} \coth\left(\sqrt{\frac{i}{X}}\right) - 1]} \tag{6}$$

Where γ is the specific heat ratio and X is function of thermal diffusivity D, as per Eq. 7.

$$X = \frac{D}{\rho R^2} \tag{7}$$

The damping coefficient is described by Eq. 8.

$$b = \frac{2\mu}{\rho\, R^2} + \frac{p_o}{2\rho\omega\, R^2} \mathrm{Imag}(\emptyset) + \frac{\omega^2 R}{2c} \tag{8}$$

And the total cavitation bubble volume is evaluated as in Eq. 9.

$$\beta = \frac{4\pi n_b R^3}{3} \tag{9}$$

Cavitation bubble volume β is also calculated from the acoustic pressure as in Eq. 10 [9] [10].

$$\beta = 2x10^{-9}P \qquad for\ p_{blake} < P < 1x10^8\ Pa. \tag{10}$$

The P_{blake} is the blake threshold and is defined as the pressure above which the cavitation bubble will implode.

Navier stokes for flow simulation:

The flow of the reactant mixture, which is assumed to be a homogeneous blend of vegetable oil and methanol is governed by the Navier-Stokes equation. A constant velocity of 0.0044 m/s is applied at the inlet for all simulations rendering the flow regime to be laminar. The velocity is selected to suit the flow rate capability of ultrasound equipments which is generally around 10 to 50 L/hr. [12].. There is however acoustic induced flow/streaming around the sonotrode due to the pressure amplitude which is neglected here. The laminar, incompressible, steady state Navier-Stokes equations are given in Eq. 11.

$$\rho(\boldsymbol{u}\nabla\boldsymbol{u}) = -\nabla P_{flow} + \mu\nabla^2\boldsymbol{u} + \rho\boldsymbol{g} \tag{11}$$

Where $\boldsymbol{u}$ is the velocity vector and μ, $\boldsymbol{g}$ are the molecular viscosity and gravitational acceleration, respectively. The obtained velocity u profile is the same as the one used in the species transport equation.

Species transport:

To analyze the reactive aspect of the process, the species transport equation is used. Which is given in Eq. 12.

$$\boldsymbol{\nabla}(-D\boldsymbol{\nabla}C_i) + \boldsymbol{u}\boldsymbol{\nabla}C_i = R_{rate} \tag{12}$$

Four species, vegetable oil, methanol, FAME (biodiesel) and glycerol are specified. C_i denotes the species, R_{rate} is the reaction rate. The reaction between vegetable oil and methanol is defined by the Arrhenius kinetics model where the rate constant is defined as in Eq.13. Though the reaction is reversible, only the forward reaction is modelled.

$$k_{flow} = A.e^{\frac{-E}{R_u.T_{liq}}} \tag{13}$$

Where E is the activation energy and R_u here is the Universal gas constant and T_{liq} is the fluid temperature. The activation energies, *E*, and pre-exponent, A, were approximated from the work of Noureddini et al. [13].

Reaction rate coupling:

The most important step in evaluating the design of the reactor is the estimation of rate constant due to sonication. This is used as a measure to judge the reactor design. The sonication reaction rate constant K_son depends on the acoustic pressure which in turn depends on the cavitation bubble volume. K_son occurs only in regions where there are cavitation bubbles, which implode upon experiencing high acoustic pressures. Therefore K_son must be a function of cavitation bubble temperature. K_son is also defined by the Arrhenius kinetic model, however the temperature is not the bulk fluid temperature, but the cavitation bubble temperature. The cavitation bubble consists of vapors of vegetable oil and methanol. Since the mixture is assumed homogeneous the vapor pressure inside the cavitation bubble is assumed as the molar average of the reactants. As per Jordens et al. [10] the cavitation bubble temperature T_{bubble} is defined as in Eq. 14. The cavitation bubble temperature is a function of the acoustic pressure (P) and vapor pressure (P_{vapor}). Applying this model assumes that the mass transfer limitations are already surpassed due to the vapor state of reactants in the bubble and the reaction is kinetically governed. Other nonlinear effects of ultrasound such as the sono-luminescence, shock waves and formation of radicals are also neglected. The K_son is given in Eq. 15.

$$T_{bubble} = \frac{T_l P(\gamma - 1)}{P_{vapor}} \tag{14}$$

$$K\_son = A.e^{\frac{-E}{R_u.T_{bubble}}} \tag{15}$$

T_L is liquid temperature but for this calculation it is assumed as 80 ^{0}C to have a vapor state of methanol.

The rate constant is an important factor for analysis of the reaction since the reaction rate is directly proportional to the rate constant. Since the sonication rate constant depends on acoustic parameters this should also reflect in the reaction rate. Hence a logical reaction rate coupling model is adopted to calculate the reaction rate, which is given by Eq. 16.

$$-R_{rate} = \left[(P > P_{blake})\beta * K_{son} * [Oil * Oil] + (1 - \beta) * k_{flow} * [Oil * Oil]\right] \tag{16}$$

The above equation ensures that K_son is only calculated when the acoustic pressure is above blake i.e. the pressure above which the cavitation bubble implodes. The second order reaction rate is as per [13].

Equivalent properties:

In all previous studies on sono-chemical reactors, the fluid medium was a single fluid. Since we extend this work to a mixture of reactants we need to estimate equivalent properties. Two properties which govern the physics largely in this study are the speed of sound and viscosity. The effective speed of sound (C) was calculated using effective bulk

modulus and density (see Eq. 17). The effective bulk modulus and density being volumetric properties were calculated using the volume fractions.

$$C = \sqrt{\frac{K_E}{\rho_E}} \tag{17}$$

Where K_E and ρ_E are equivalent bulk modulus and equivalent density.

For calculating equivalent viscosity the Refutas equation was used. In this method the viscosity blend indices for the reactants are calculated as per Eq. 18. Using mass fractions the blend index of the mixture is calculated as per Eq. 19 and finally the effective viscosity is calculated from Eq. 20.

$$VBN_i = 14.534 \times \ln(\ln(\nu_i + 0.8)) + 10.975 \tag{18}$$

$$VBN_{mixture} = \sum_{i=0}^{N} x_i \times VBN_i \tag{19}$$

$$\nu_{mixture} = \exp[\exp\left(\frac{VBN_{mixture} - 10.975}{14.534}\right)] - 0.8 \tag{20}$$

Where VBN is the viscosity blend index, ν_i is the kinematic viscosity of the element in cSt, and x_i is the mass fraction. Other properties like surface tension and thermal diffusivity are taken for methanol.

Boundary conditions

The initial pressure amplitude P= P_w was assigned as a dirichlet boundary condition at the sonotrode tip implying the source of ultrasound energy dissipation, where P_w is a function of the rated power P_d as given in Eq. 21

$$P_w = \sqrt{\frac{2\rho C P_d}{S}} \tag{21}$$

S here is the area of the sonotrode tip (transducer). For all other walls a sound absorbing boundary condition P=0 was applied implying Teflon material.
For the flow simulation the velocity boundary condition was applied at the inlet, and dirichlet P_{flow}=0 was applied at the outlet. All walls were subjected to no slip, u=0 boundary condition. For species transport the inflow was given as molar concentrations. All simulations were carried out at constant molar ratio of 3 to 1 (methanol to oil). All properties are given in Table. 1.

RESULTS AND DISCUSSION

There are two aspects of the simulation that must be understood, critiqued and questioned to comprehend the design analysis. The first aspect is the acoustic pressure and its distribution in the reactor volume, which can be constituted as the physical aspect. The second aspect is the reactive or chemical aspect, which is represented by the rate constant K_son which again is governed by the acoustic pressure and cavitation bubble temperature. The acoustic pressure distribution must spread over all regions of the reactor to make the most of the available acoustic energy. Major

factors that affect these aspects of the reactor are the fluid density, reactor material, reactor geometry, rated power, and frequency. The fluid considered here is a mixture of vegetable oil and methanol. The reactor material is Teflon, which is characterized as sound absorbing material [9]. Using reflective materials like steel, causes wave reflection inside the reactor.

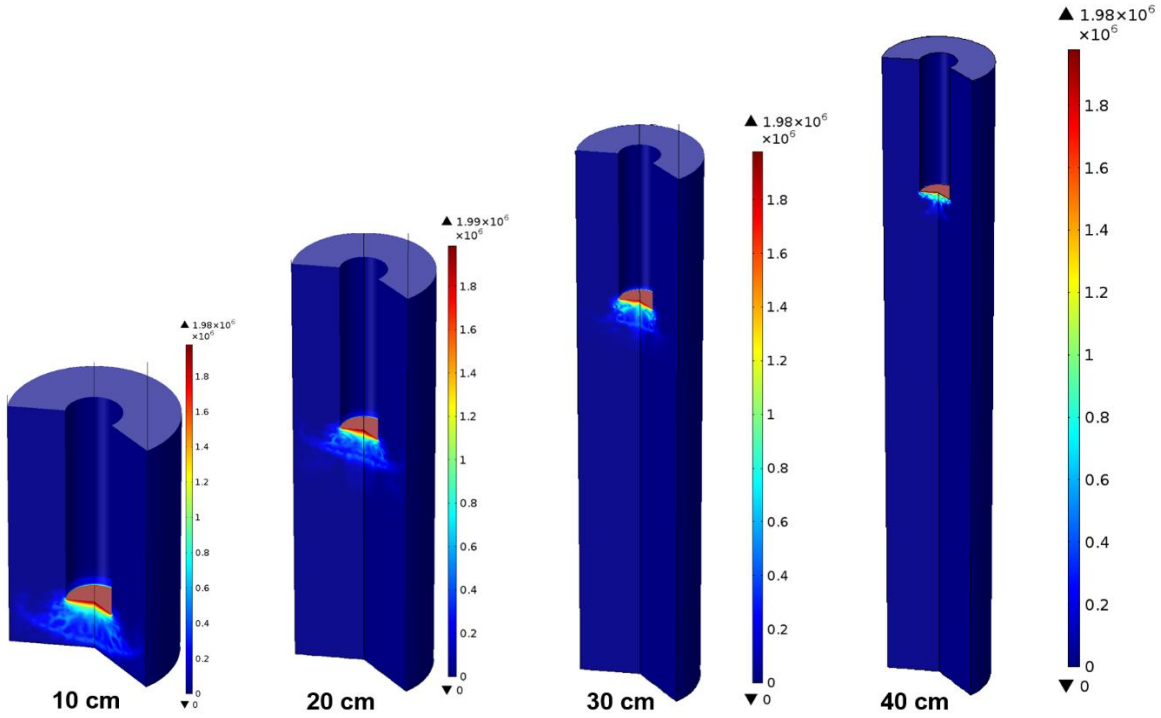

Fig.2 Absolute acoustic pressure (Pa) distribution at different heights, 500 W, 24000 Hz.

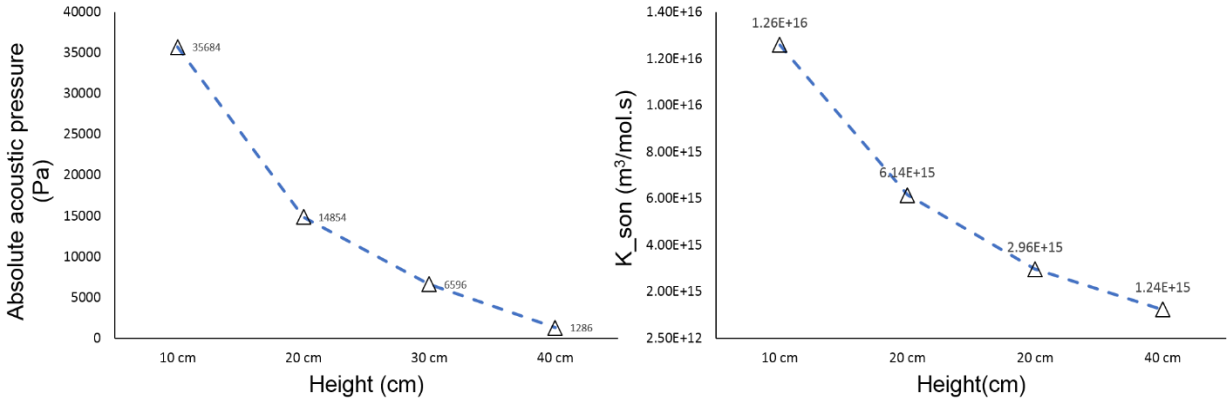

Fig.3 (left) Volume averaged absolute acoustic pressure (Pa); (right) volume averaged sonication rate constant at different heights.

Wave reflections inside the reactor generate heat. The ultrasound sonotrodes are generally designed to turn off once the temperatures reach a certain threshold. Extreme temperatures may even damage the sonotrode tips. Hence in some application it requires high external cooling, which adds to the costs. Optimization of reactor geometry is one good way to achieve a better design. The height and diameter of the cylindrical reactor in this study were varied individually. While geometry and rated power affect the boundary conditions of the reactor and the sonotrode, the frequency is the only parameter that affects the governing Helmholtz equation. The frequency is used to calculate the complex wave number hence its variation affects the real and imaginary parts of the complex wave numbers. Acoustic pressure and K_son

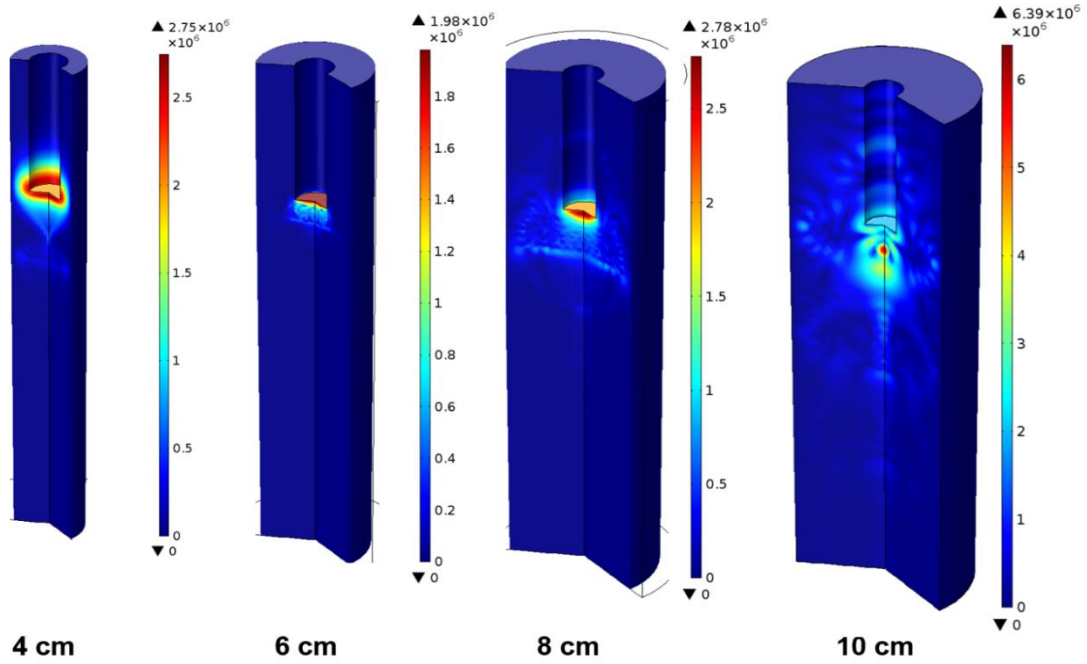

Fig.4 Absolute acoustic pressure (Pa) distribution at different diameters, 500 W, 24000 Hz.

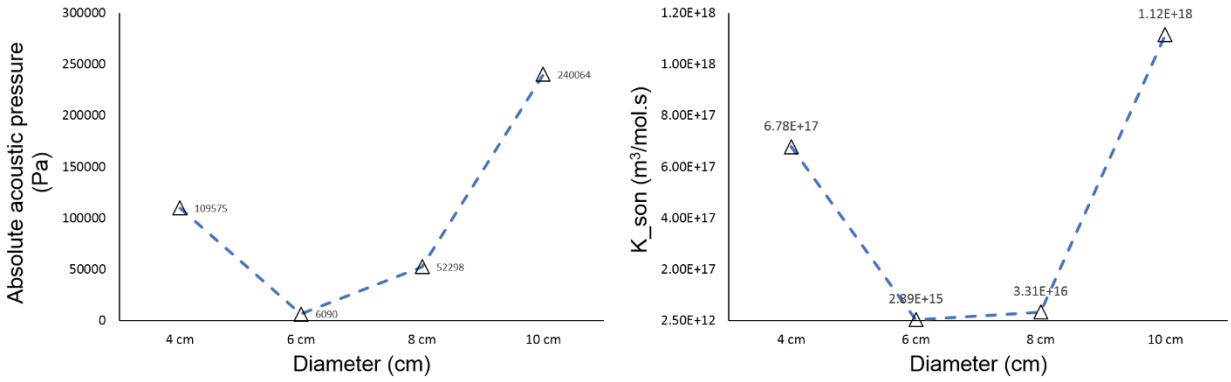

Fig.5 (left) Volume averaged absolute acoustic pressure (Pa); (right) volume averaged sonication rate constant at different diameters.

are the two resultants that are studied by carrying out the sensitivity analysis. Based on them the optimized design is selected.

Sensitivity study

Effect of height:

The height was varied from 10 cm to 40 cm in steps of 10 cm. The simulation was carried out at the rated power of 500 W and a frequency of 24,000 Hz. The diameter was set at 6 cm. The peak acoustic pressure obtained in all the

cases was more or less similar at 1.98 MPa. Fig.2 shows the contour plots of the acoustic pressure distribution at different heights and Fig. 3 shows the line plot of the volume averaged acoustic pressure as well as the K_son.

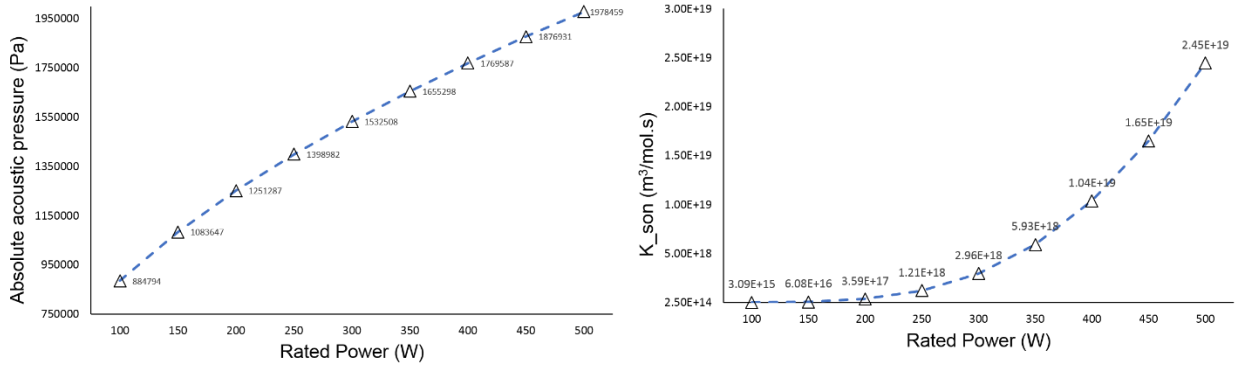

Fig.6 (left) Peak absolute acoustic pressure (Pa); (right) sonication rate constant at different powers, 24000 Hz, 30 cm height and 6 cm diameter.

Due to cavitation bubble attenuation, higher acoustic pressures were observed in regions close to the sonotrode. To normalize the changes in volume among the cases the volume averaged acoustic pressure was studied. As the height increased the volume averaged acoustic pressure decreased. It can be clearly noticed from Fig. 2 that for taller reactors, the lower regions of the reactor experienced much less acoustic activity obviously due to the attenuation from the cavitation bubbles. The best acoustic pressure (volume averaged) was for the reactor with 10 cm height and it was 36 kPa and the least was 1.3 kPa for the height of 40 cm.

K_son results also showed similar variations as the volume averaged acoustic pressure. The maximum cavitation bubble temperature for these cases was close to 2,700 K. Volume averaged K_son values were studied, which also reduced with increasing height. The maximum K_son (volume averaged) for this study was 1.26e16 m^3/mol.s and the least was 1.24e15 m^3/mol.s. In comparison with the K_son, K_flow, which is the rate constant from flow agitation, was numerous orders lower at 5.6e-6 m^3/mol.s. K_flow did not vary largely with the changes in height. This shows clear superiority of sonicated transesterification. The results of acoustic pressure and K_son point out the advantage in keeping the reactor shorter. But shorter reactors also mean smaller control volumes or less volume of fluid sonicated. Therefore to retain the height we need to optimize other parameters.

Effect of diameter:

The diameter was varied from 4 cm to 10 cm in steps of 2 cm. The rated power governs the initial pressure amplitude at the sonotrode tip. The simulation was carried out at a rated power of 500 W and frequency of 24,000 Hz. The length of the reactor was fixed at 30 cm. Fig. 4 shows the acoustic pressure distribution for different diameters. Fig 5. show the volume averaged acoustic pressure and K_son.Contrary to what was observed in the case of height variation, the acoustic pressure did not decrease with increase in diameter. For the cases of diameters 8 cm and 10 cm the acoustic pressure distribution was more widespread, whereas for the diameters of 4 cm and 6 cm the acoustic pressure was concentrated close to the sonotrode due to their narrower design. This behavior is caused by two reasons, the first being the cavitation bubble cloud. The attenuation is more prominent in the vertical axis as compared to the radial axis. The second reason are the sound absorbing boundaries. The acoustic pressure at the boundaries is absorbed by the walls. When the walls are closer to the sonotrode most of the acoustic energy is absorbed. With larger diameters more fluid is exposed to the acoustic energy hence the pressure distribution is widespread. It is also noticed that with varying diameter the cavitation profiles tend to be more complex and lack a well-defined relation with the diameter increase. This fact is reflected in the quantities of the volume averaged acoustic pressures. The least value of 6.1 kPa was observed for the diameter of 6 cm and the largest value of 240

kPa was seen with diameter of 10 cm. However their distribution profiles do increase in spread with increase in diameter. The peak acoustic pressure was maximum with 10 cm diameter at 6.4 MPa.

K_son variation with diameter adhered to the same profile of the volume averaged acoustic pressure. The least K_son value of 2.9e15 m^3/mol.s was seen at diameter of 6 cm, and the highest of 1.2e18 m^3/mol.s was seen at diameter of 10 cm. The maximum cavitation bubble temperature in this study was 8,827 K (at 10 cm diameter). K_flow was again several times lower at 5.6e-6 m^3/mol.s which did not change much with diameter. The results from this analysis show that having larger diameters can be beneficial under the considered boundary conditions. However much larger diameters call for higher flow rates. These results are suitable for sonication equipments which can process fluids with flow rate of 10 to 50 L/hr.

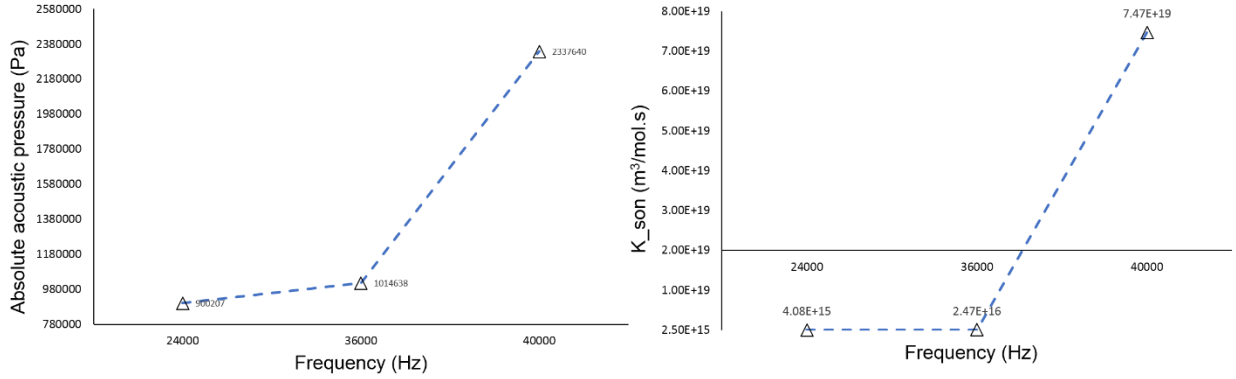

Fig.7 (left) Peak absolute acoustic pressure (Pa); (right) sonication rate constant at different frequencies, 100 W, 30 cm height and 8 cm diameter.

Effect of rated power:

The rated power was varied from 100 to 500 W in steps of 50 W. The frequency was 24,000 Hz. The diameter was 6 cm and height was 30 cm. Fig 6 shows the variation of peak acoustic pressure and K_son (volumetric maximum) with rated power.The acoustic pressure showed a direct relation with the rated power. As the rated power increased the acoustic pressure also increased. The maximum, peak acoustic pressure of 1.9 MPa was seen at 500 W power and the least of 0.88 MPa was at a power of 100 W. The cavitation bubble temperature and K_son being functions of acoustic pressure also followed the same trend. Highest cavitation bubble temperature was 2,700 K (at 500 W) and least was 1,200 K (at 100 W). At the lowest power the volumetric maximum value of K_son was 3.1e15 m^3/mol.s and at the highest power setting it was 2.5e19 m^3/mol.s.

Effect of frequency:

In this study three frequencies i.e. 24,000 Hz, 36,000 Hz and 40,000 Hz are considered. The diameter was 8 cm and height was 30 cm. The rated power was 100 W. Fig. 7 shows the variation in peak acoustic pressure and K_son with frequency.The results showed increasing values of peak acoustic pressure and K_son with increase in frequency. However the result did not seem to be directly proportional to the frequency value. The gain in peak acoustic pressure between 24,000 Hz and 36,000 Hz was lower than the gain between 36,000 Hz and 40,000 Hz. This unpredictable variation is due to the change in the complex wave number, which is iteratively calculated in the model. In addition to this the change in cavitation bubble volumes with varying frequency also affects the acoustic pressure. The least acoustic pressure was 0.9 MPa at 24,000 Hz and highest was 2.3 MPa at 40,000 Hz. The least

K_son was 4.8e15 m^3/mol.s (24000 Hz, Tmax = 1243 K) and maximum at 7.5e19 m^3/mol.s (40,000 Hz, Tmax = 3,127 K).

CONCLUSION

In this work a design for continuous sonochemical reactor for biodiesel production from vegetable oils was evaluated through numerical modelling. The ultrasound wave was simulated with the Helmholtz equation. A complex wave number was used to account for the attenuation due to cavitation bubbles. Coupled Navier-Stokes and species equation were used to model the reactive flow. The Arrhenius kinetic principle was used to evaluate the reaction kinetics of the flow and also the bubble. A sensitivity analysis based on height, diameter, rated power and frequency was carried out to optimize the acoustic and reactive characteristics of the reactor. The height was varied from 10 cm to 40 cm in steps of 10 cm. The diameter was varied from 4 cm to 10 cm in steps of 2 cm. The power was varied from 100 to 500 W in steps of 50 W. Three frequencies, 24000 Hz, 36000 Hz and 40000 Hz were considered. The acoustic pressure and sonication rate constant were extensively analyzed in all these cases. It was observed that for taller reactors, the acoustic activity did not reach to the lower region of the reactor due to attenuation from cavitation bubbles. But for increase in diameter the acoustic pressure distribution was wide spread implying lower attenuation in radial direction. Acoustic pressure increased with increase in rated power. For frequency increase, the acoustic pressure increased but with some unpredictability. The reaction rate constant for sonication showed similar results as acoustic pressure in all cases due to its dependency on acoustic pressure. The sonication rate constant was multiple orders higher than the rate constant of flow. The analysis was based on an approximate fluid flow rate of 10 L/hr. hence the results are suitable for this range of flow rate, which is what is generally the capacity of sonotrode ultrasound equipment in market. For the current study we found an optimized design with 10 cm diameter, 30 cm height. At this geometric condition the acoustic pressure and K_son were observed to be the highest. It is seen that having a larger diameter helps in overcoming the attenuation losses in taller geometries, this allows for having a larger fluid process volume. These results are applicable only for biodiesel production, for other process fluids the performance patterns may change.

Table 1 Property Table

Property	**Unit**	**Value**
Activation energy, E	J/Mol	164958.4
Adiabatic coefficient, γ	-	1.4
Ambient liquid pressure, P_{liq}	Pa	1.00E+05
Blake threshold P_{blake}	Pa	1.00E+05
Oil density [14]	Kg/m^3	883
Dynamic viscosity of oil [15]	Pa.s	1.62E-02
Density of methanol [16]	Kg/m^3	883
Dynamic viscosity of methanol [17]	mPa.s	0.545
Pre-exponential factor A	m^3/mol/s	3.49E+22
Vapor pressure of vegetable oil [18]	Pa	543
Vapor pressure of methanol[19]	Pa	13020

Universal gas constant R_u	J/mol.K	8.314
Bulk modulus of Methanol [20]	N/m^2	0.8E9
Bulk modulus of Oil [21]	N/m^2	2.1E9
Surface tension of methanol, σ [22]	N/m	0.002250
Thermal diffusivity of the methanol, D [23]	m^2/s	5.9E-08

REFERENCES

[1] Gerpen J. V.: Biodiesel processing and production. Fuel Processing Technology. 86. 1097-1107 (2005).

[2] Gude V. G., Grant G. E.: Biodiesel from waste cooking oils via direct sonication. Applied Energy. 109, 135-144 (2013).

[3] Stavarache C., Vinatoru M., Maeda Y.: Ultrasonic versus silent methylation of vegetable oils. Ultrasonics Sonochemistry. 13, 401-407 (2005).

[4] Manickam S., Arigela V. N. D., Gogate P. R.: Intensification of synthesis of biodiesel from palm oil using multiple frequency ultrasonic flow cell. Fuel Processing Technology. 128, 388-393 (2014).

[5] Babajide O., Petrik L., Amigun B., Ameer F.: Low-cost feedstock conversion to biodiesel via ultrasound technology. Energies, 3, 1691-1703 (2010)

[6] Gogate P. R., Sutkar V.S, Pandit A. B., Sonochemical reactors: important design and scale up considerations with a special emphasis on heterogeneous systems, Chem. Eng. J. 166, 1066–1082 (2011).

[7] Sutkar V.S, Gogate P. R..: Design aspects of sonochemical reactors: Techniques for understanding cavitational activity distribution and effect of operating parameters. Chem. Eng. J. 155, 26-36 (2009).

[8] Wei Z., Weavers L. K.: Combining COMSOL modeling with acoustic pressure maps to design sono-reactors. Ultrasonics Sonochemistry. 31,490-498 (2016).

[9] Jamshidi R., Pohl B., Peuker U.A., Brenner G.: Numerical investigation of sonochemical reactors considering the effect of inhomogeneous bubble clouds on ultrasonic wave propagation, Chem. Eng. J. 189–190 (2012).

[10] Jordens J., Honings A., Degrève J., Braeken L., Tom Van Gerven.: Investigation of design parameters in ultrasound reactors with confined channels. Ultrasonics Sonochemistry. 20, 1345-1352 (2013).

[11] Commander K.W., Prosperetti A., Linear pressure waves in bubbly liquids: comparison between theory and experiments, J. Acoust. Soc. Am., 85, 732–746 (1988).

[12] Hielscher equipments https://www.hielscher.com/400s_p.htm.

[13] Noureddini H., Zhu D.: Kinetics of Transesterification of Soybean Oil. Journal of the American Oil Chemists Society. 74, 1457-1463 (1997).

[14] Nikoli B. D., Markovi B. K., S. D., Mitrovi M. S.: Determining the speed of sound, density, and bulk modulus of rapeseed oil, biodiesel, and diesel fuel. Thermal Science. 16, 505-514 (2012).

[15] Fasina O. O., Z. Colley.: Viscosity and specific heat of vegetable oils as a function of temperature: 35°C to 180°C. International Journal of Food Properties. 11, 738–746, (2008).

[16] Lyde D. R..: CRC Handbook of Chemistry and Physics (2005).

[17] González, B.: Density, dynamic viscosity, and derived properties of binary mixtures of methanol or ethanol with water, ethyl acetate, and methyl acetate at T = (293.15, 298.15, and 303.15) K . The Journal of Chemical Thermodynamics. 39, 1578–1588. (2007).

[18] Ndiaye P. M., Tavares F. W., Dalmolin, I. Dariva C., Oliveira D., Oliveira J. V.: Vapor Pressure Data of Soybean Oil, Castor Oil, and Their Fatty Acid Ethyl Ester Derivatives. J. Chem. Eng. Data, 50, 330-333, (2005).

[19] Gibbard H. F., Creek J. L.: Vapor pressure of methanol from 288.15 to 337.65 K. J. Chem. Eng. Data, 19, 308–310 (1974).

[20] Nesbitt B.: Handbook of pumps and pumping. (2006).

[21] Nikolic B. D., Breda K. E. G. L., Markovic S. D., Mitrovic M. S.: Determining the speed of sound, density, and bulk modulus of rapeseed oil, biodiesel, and diesel fuel. Thermal science 16 (2012).

[22] Surface tension values of some common test liquids for surface energy analysis. http://www.surface-tension.de/ (2006).

[23] Bailey R. T., Cruickshank F.R., Pugh D., Weir I.J.M.: The thermal diffusivity and thermal conductivity coefficient of methanol vapor, 134, 311-315 (1987).